

Fig. 8. A comparison of SWE and Gaussian techniques for determining  $R_2$ .

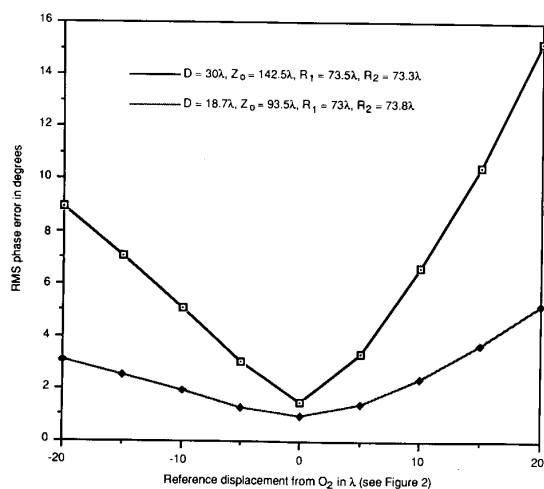


Fig. 9. Sensitivity of phase error at  $A_2$  with referenced phase center—rms phase error.

spacing of  $Z_0 = 142.5 \lambda$ , there is little control of defocusing for small reflectors (e.g., diameters less than  $30 \lambda$ ).

Fig. 8 shows a comparison of the radius of curvature computed from the SWE technique and the corresponding value obtained from the Gaussian beam analysis [3]. The agreement between the two is poor for large values of  $R_1$  wherein the paraxial ray approximation of the Gaussian technique does not hold well.

Fig. 9 illustrates the variation of root mean square phase error for an apparent phase reference point that is displaced from the best-fit phase center  $O_2$ . For a given value of the spacing  $Z_0$ , the variation of rms phase error is more rapid for larger diameter reflectors. For small sized reflectors we have a relatively diffused focusing. Hence for a "small" reflector system, the overall gain of a beamwaveguide-fed reflector antenna is relatively less sensitive to defocusing. Experimental measurements on NASA/JPL beamwaveguide antennas confirm these results.

#### IV. CONCLUSION

This communication has presented an analysis of amplitude and phase shaping effects on the spillover loss and the defocusing

characteristics of reflector beamwaveguides. Diffraction effects of propagation between two reflectors have been modeled by a fast spherical wave expansion technique. Numerical results indicate that for aperture sizes less than  $30 \lambda$ , there is insufficient control on defocusing due to amplitude and phase shaping. Design trade-offs on spillover loss and defocusing are possible by changing the amplitude and phase distribution of the input wavefront for larger size apertures.

#### ACKNOWLEDGMENT

The authors would like to thank D. T. Veruttipong for many useful discussions during the course of this work.

#### REFERENCES

- [1] M. Mizusawa and T. Kitsuregawa, "A beamwaveguide feed having a symmetric beam for Cassegrain antennas," *IEEE Trans. Antennas Propagat.*, vol. AP-21, pp. 844-846, Nov. 1973.
- [2] T. Veruttipong, J. R. Withington, V. Galindo-Israel, W. A. Imbriale, and D. Bathker, "Design considerations for beamwaveguide in the NASA deep space network," *IEEE Trans. Antennas Propagat.*, vol. 36, pp. 1779-1787, Dec. 1988.
- [3] H. Kogelnik, "Imaging of optical modes—Resonators with internal lenses," *Bell Syst. Tech. J.*, vol. 44, pp. 455-494, Mar. 1965.
- [4] T.-S. Chu, "An imaging beamwaveguide feed," *IEEE Trans. Antennas Propagat.*, vol. AP-31, pp. 614-619, July 1983.
- [5] —, "Geometrical representation of Gaussian beam propagation," *Bell Syst. Tech. J.*, vol. 45, pp. 287-299, 1966.
- [6] V. Galindo-Israel, W. A. Imbriale, and R. Mittra, "On the theory of the synthesis of single and dual offset shaped reflector antennas," *IEEE Trans. Antennas Propagat.*, vol. AP-35, pp. 887-896, Aug. 1987.
- [7] R. Padman, J. A. Murphy, and R. E. Hills, "Gaussian mode analysis of Cassegrain antenna efficiency," *IEEE Trans. Antennas Propagat.*, vol. AP-35, pp. 1093-1103, Oct. 1987.
- [8] G. A. J. van Dooren, "Quasi-optical analysis of a multireflector demultiplex circuit using Gaussian beams," ESTEC Working Paper 1565, p. 1, European Space Agency, Noordwijk, the Netherlands, Oct. 1989.
- [9] A. C. Ludwig, "Spherical wave theory," in *Handbook of Antennas Design*, A. W. Rudge *et al.*, Eds. London, U.K.: Peregrinus, 1982, sec. 2.3.

### Experimental Verification of the 2-D Rooftop Approach for Modeling Microstrip Patch Antennas

Robert A. York, Richard C. Compton, and Barry J. Rubin

**Abstract**—Radiation pattern and input impedance measurements for a rectangular microstrip patch are used to establish the accuracy of a general moment method approach. The approach uses two-dimensional (2-D) rooftop basis functions to model arbitrarily shaped, three-dimensional (3-D) composite, conductor-dielectric structures. The numerical results show agreement with the measurements. However, both the experimental and theoretical results show considerable differences when

Manuscript received July 6, 1990; revised December 26, 1990. The work performed at Cornell University was supported by the U. S. Army Research Office and an IBM grant.

R. A. York and R. C. Compton are with the School of Electrical Engineering, Cornell University, Ithaca, NY 14853.

B. J. Rubin is with the IBM T. J. Watson Research Center, Yorktown Heights, NY 10598.

IEEE Log Number 9143726.

compared with previously published analyses using pulse-basis functions. These differences and others that are pointed out cast serious doubts on the validity of using pulse basis functions to model scattering or radiation from composite structures.

## I. INTRODUCTION

Theoretical studies have demonstrated the use of subsectional basis functions to model the volume polarization current in dielectric structures for scattering analysis [1]–[6]. Recently this approach has been extended to handle composite conductor-dielectric structures; in [7], the scattered field from conductor-dielectric structures is calculated, and in [8], [9] the far-field pattern of a microstrip patch antenna is calculated. The advantage of the polarization-current approach is that the structures can have arbitrary shape, and this permits the analysis of structures that have finite-size dielectric regions. However, [8, fig. 2], [9, fig. 9], which are based upon the use of pulse-basis functions, display radiation patterns that do not agree with our results or with published experimental results for a similar structure [10], especially below the ground plane of the patch. Under further scrutiny the scattering results for composite structures where the dielectric and metal are in contact [7] were also found to be in error, based upon comparisons with numerical results from our approach. A further search of the literature reveals a number of publications that point to problems with the accuracy of pulse functions [11]–[13] for modeling even purely dielectric structures.

An alternative approach uses 2-D rooftop functions to model both the volume polarization current in the dielectric and the surface current on the conductors [14]. This approach should be superior to the pulse-basis approach [1]–[4], [7]–[9] because rooftop functions avoid the fictitious charge produced by pulse functions [15]. The accuracy of the 2-D rooftop approach has been previously verified by comparing calculated results with other published theoretical approaches, and through extensive numerical convergence studies [14]. In this communication, input impedance and antenna pattern measurements are used to look more closely at the accuracy of this method. A rectangular microstrip patch was studied to enable a direct comparison with the results of [8]. The experimental work confirms the use of 2-D rooftop functions, and casts doubt on the validity of using pulse functions for modeling composite conductor-dielectric structures.

## II. MODELING APPROACH

The structure under consideration is shown in Fig. 1, with dimensions chosen to match those of [8]. The patch is modeled using a moment method technique. First, each dielectric region is replaced by an equivalent region that consists of a 3-D array of thin-wall sections, as described in [14]. This allows the 2-D rooftop functions to represent both the polarization current in the dielectric regions and the surface current on the conductors. The electric field boundary conditions are then applied, over both the dielectric thin-walls and the conductors, through the use of surface impedances. Fig. 2 illustrates the use of the thin-wall sections to model the dielectric region, and the use of rooftop functions to model the currents. In Fig. 2, a patch antenna structure is subdivided into a  $3 \times 3 \times 2$  grid. Two surface impedances are associated with each thin-wall section, one for each orthogonal direction in the plane of the section. The approach is described in detail in [14]. Consistent with the discussion in [14], for this particular structure, only half-rooftop functions are used to represent the polarization and surface currents. Corresponding half-rooftop functions are subsequently combined, by making their coefficients dependent, to form corner functions so that current at each corner is continuous and the

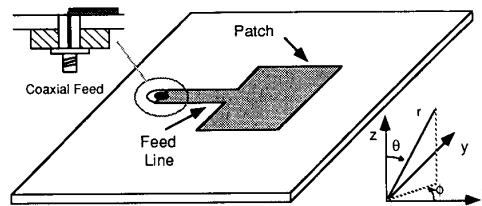


Fig. 1. Microstrip patch geometry. The patch is 5 cm by 5 cm and is symmetrically fed by a 1 cm wide and 5 cm long transmission line. The patch/feed are centered on a  $93 \pm 5$ -mil-thick substrate having sides 20 cm along  $x$  and 15 cm along  $y$ , with  $\epsilon_r = 2.33 \pm 0.02$ . A second structure with substrate 40 cm along  $x$  and 10 cm along  $y$  was also studied. Both structures include finite-size ground planes which cover the entire backside of the substrate.

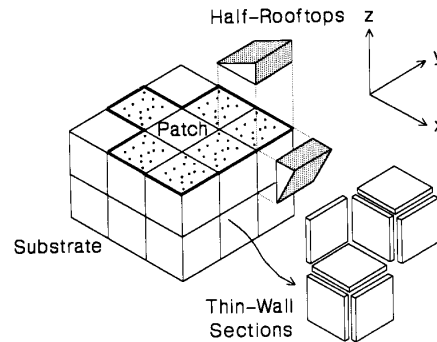


Fig. 2. Diagram indicating the use of thin-wall sections and rooftop functions to model the current density in a structure including a conductive patch.

net current at each junction of thin-wall regions is zero. This procedure prevents generation of fictitious charges that would otherwise lead to numerical problems. A matrix equation is generated and solved in standard fashion. Good agreement with previously published results and consistency with physical principles have been demonstrated in [14]. However, patch antennas were not considered in those references, through microstrip lines, dielectric cubes, and other composite structures were analyzed. This same approach has also been applied to spiral-shaped patch antennas [16] and guided-wave problems that involve finite-size dielectric regions [17]. In the latter references, 2-D and 3-D waveguides were analyzed, including coaxial, microstrip, and dielectric structures.

The computer code based on the algorithm given in [14] can be used for any structure that can be defined by steps along a Cartesian coordinate system. The number of independent current elements is currently limited to about 6000 because of run time and storage constraints. Though not a fundamental limitation, the grid must be uniform along the  $x$ ,  $y$ , and  $z$  directions; the use of such a uniform grid allows table-lookup and other procedures that drastically reduce the computer time necessary to fill in the elements of the resulting matrix equation. In particular, a grid of  $20 \times 30 \times 1$  was used for the first structure, and a grid of  $40 \times 20 \times 1$  for the second structure (Fig. 1). Because the substrate is thin compared to the wavelength, only one subsection along  $z$  for this structure is needed; one subsection allows for a linear variation of polarization current along this direction. Symmetry about the  $y$  direction allows a factor of two reduction in matrix size; for the smaller substrate, 3334 independent current elements are required (run time is about 50 min per frequency point, using an IBM Mod 600 vector processor unit), and 4449 elements are required for the larger substrate.

Consistent with other moment formulations, the patch antenna is

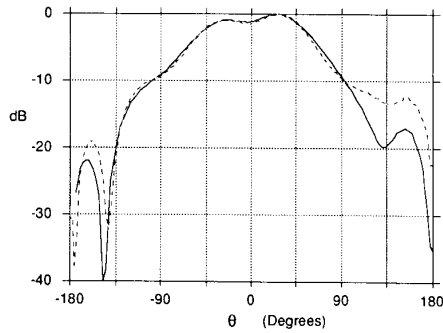


Fig. 3. Calculated (solid line) and measured (dashed) pattern for the  $E$ -plane ( $E_\theta$ ) for the  $20\text{ cm} \times 15\text{ cm}$  patch in Fig. 1. Note that rectangular plots have been used because they accentuate small differences in the sidelobe levels that are difficult to see in a polar plot.

excited by a 1 V source placed across a delta gap in one of the conducting segments [18]. In the patch structures discussed here, that source is placed in a short rectangular segment, having zero thickness and the same width as the feed line, that runs from the ground plane to the left end of the feed line shown in Fig. 1. In the formulation, the source location can only be specified to within one-half a subsection. For the aforementioned grids, the subsection sizes are 1.0 cm along  $x$ , 0.5 cm along  $y$ , and the substrate thickness, or 0.236 cm, along  $z$ .

### III. MEASUREMENTS

A variety of patch feed arrangements were tried both experimentally and theoretically. All gave similar patterns except at large angles  $\theta$  (near  $\pm 180^\circ$ ) where the detected signal levels were small. A backside feed through the substrate (Fig. 1) was found to give the most reproducible results for large angles. A flange mount jack receptacle was used to transition from coaxial cable to the feed line (Omni-Spectra part 2052-1200-00, inner diameter 50 mil and outer diameter 162 mil), and was attached to the ground plane with an aluminum block as shown in Fig. 1. The signal transmitted by the patch is received by a 20 dB rectangular horn spaced six free-space wavelengths from the patch. The close proximity of the horn and patch were simulated in the modeling and found not to significantly change the pattern from the far-field pattern.

Initially the patch antennas were made with copper adhesive tape placed on single sided copper clad Duroid RT5870 circuit board. It should be noted that the resistive losses at 5 GHz of the copper tape may be up to 10 times greater than for boards with cladding on both sides, due to the nature of the nonconducting tape adhesive. Including a resistance 10 times greater than bulk copper, however, was found to change the computed results only slightly. To further confirm this, a patch was etched on a two-sided copper board and the impedance measurements did not change significantly.

$E$ -plane ( $\phi = 0^\circ$ ,  $\theta = [-180^\circ, +180^\circ]$ ) and  $H$ -plane ( $\phi = 90^\circ$ ,  $\theta = [-180^\circ, +180^\circ]$ ) patterns at 1.875 GHz for the smaller substrate are shown in Figs. 3 and 4. This particular frequency was chosen because it corresponds to the 16 cm free-space wavelength used in [8]; it is also close to the patch resonance. The agreement for the backside radiation in the  $H$ -plane is not as good as in the  $E$ -plane, because the measured field was found to be extremely sensitive to the alignment of measurement setup. This behavior was also observed in the simulations, but was not as pronounced. The metal block used to secure the coaxial connector under the ground plane (inset Fig. 1) may be a source of error in the backside radiation patterns.

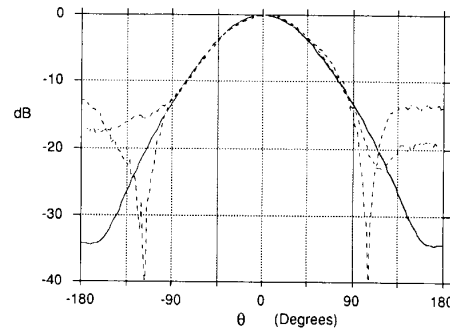


Fig. 4. Calculated (solid line) and measured (dashed) pattern for the  $H$ -plane ( $E_\phi$ ) for the  $20\text{ cm} \times 15\text{ cm}$  patch in Fig. 1. For this plane only, measurements and calculations showed that sidelobe levels are very sensitive to alignment of the antenna and horn. Two measurements with the alignment changed slightly are displayed to illustrate this.

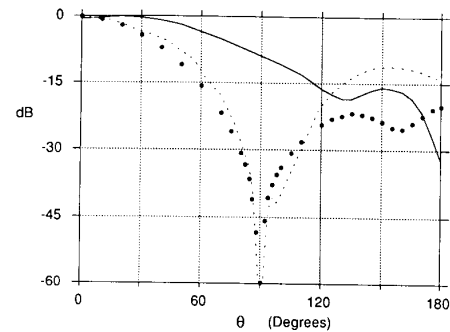


Fig. 5.  $E$ -plane plot showing discrepancies between rooftop calculation (solid line) and [8] (dashed) for the  $20\text{ cm} \times 15\text{ cm}$  patch in Fig. 1 with  $\epsilon_r = 2.56$ . Solid circles indicate rooftop calculations for  $\epsilon_r = 1.0$ .

The results of Figs. 3 and 4 differ significantly from those presented in [8], which show a null in the  $E$ -plane pattern at  $\theta = 90^\circ$ . The measured structure in this paper differs from that in [8] only in the manner in which the patch is fed and slightly in the value of the relative dielectric constant of the substrate ( $\epsilon_r = 2.56$  in [7] against  $\epsilon = 2.33$  here). However, numerical studies, which include the ideal feed of [8] and the slightly higher dielectric constant substrate, show that this does not significantly change the pattern and so cannot account for the discrepancy. Qualitative experimental agreement with our results is also given in [10, fig. 9] which considers a similar structure operated at a frequency, like ours, near the patch resonance.

The errors in [8], [9] may be due to a fundamental limitations in the use of pulse functions, an error in computer code or numerical inaccuracies. However, since the scattering results in [7, figs. 3–6] could not be duplicated, even qualitatively, with the rooftop approach, there appears to be a serious shortcoming in the use of pulse functions for modeling composite structures. An interesting, perhaps related issue, is the ability of the pulse functions to represent the polarization current in composite structures, at least for the given grid. A patch structure having a relative dielectric constant of unity (i.e., horizontal conductors in free space) would have a null at  $\theta = 90^\circ$ , since horizontal currents alone cannot give a far-field contribution at this angle and polarization. Calculations for a patch in which  $\epsilon_r = 1$  show the same basic features as the results in [8], which is a null in the  $E$ -plane ( $E_\theta$ ) at  $90^\circ$  and a single valley in the  $H$ -plane ( $E_\phi$ ), as shown in [8, fig. 2]. Fig. 5 compares our results with those presented in [8], as well as our calculations for a patch

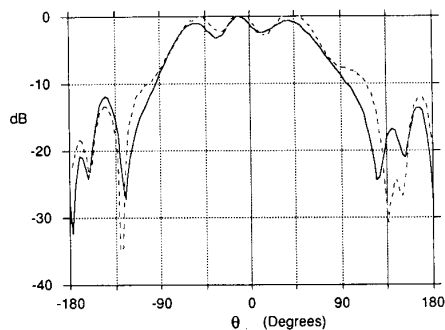


Fig. 6. Calculated (solid line) and measured (dashed) pattern for the  $E$ -plane ( $E_\theta$ ) for the 40 cm  $\times$  10 cm patch in Fig. 1.

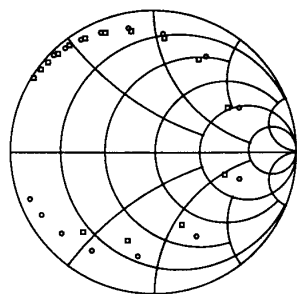


Fig. 7. Calculated reflection coefficient data (circles) compared with measurements (squares) over the range 2.0 to 2.7 GHz. A 3.75 cm  $\times$  2.5 cm patch was used for this figure, with a backside coaxial feed. No fitted parameters were used in this plot.

structure with  $\epsilon_r = 1$ . The resemblance between the last two curves supports our suspicion that the pulse functions are not properly representing the polarization current in the dielectric.

Fig. 6 shows measured and calculated patterns for the larger substrate (40 cm  $\times$  10 cm). Ripples in the pattern at small angles are consistent with surface-wave resonances and/or diffraction at the edges of the substrate [21], [22]. Note that this behavior is accurately predicted by the analysis.

The pattern agreement (Figs. 3, 4, and 6) indicates that the modeling technique yields reliable results for far-field quantities, but does not provide information on the validity of the near fields. Near-field quantities can be tested by looking at the antenna feed impedance. Measurements of the feed impedance  $Z_{\text{feed}}$  were performed by measuring the reflection coefficient  $\rho$  of the patch with an HP 8510 network analyzer,  $\rho = (Z_{\text{feed}} - Z_0)/(Z_{\text{feed}} + Z_0)$ . Fig. 7 shows good agreement between theory and experiment for the reflection coefficient of a 3.75 cm  $\times$  2.5 cm patch, centered on a 6.25 cm  $\times$  5 cm substrate, and with a backside coaxial feed 0.9275 cm from the edge of the patch. The reference plane for the measurement coincides with the ground plane. No fitted parameters or additional reactances were added to the measurements in Fig. 7.

#### IV. DISCUSSION

The rooftop approach for modeling polarization currents for patch antenna structures yields results which agree well with experiment. The impedance, which relies on an accurate representation of the near field, was shown to agree reasonably well with theory even at frequencies where only four sections per wavelength in the dielectric are employed. Agreement for the  $E$ -plane patterns were obtained for both structures considered. Though the agreement for the  $H$ -plane was good for  $-90 \leq \theta \leq 90$ , there were differences out-

side this region, where the nulls exist. However, in this region the  $H$ -plane is very sensitive to the alignment (Fig. 4) and each time the patch is slightly shifted the depth and positioning of the measured nulls change noticeably. This effect was also observed in the simulations. A few decibel variation in the calculated  $H$ -plane was observed when the angle  $\phi$  was varied from  $90^\circ$  to  $92^\circ$ . Thus, the measurement of the  $H$ -plane in this region should be given far less weight than the measurement of the  $E$ -plane, which is not as sensitive to alignment. Based on the disagreement in results between the rooftop approach and the pulse function approach, the technique described in [8], [9] appears to have limitations for the patch on a dielectric.

The impedance calculation, as given in Fig. 7, is computationally expensive because of the large number of rooftop currents and frequencies required. However, the input impedance for the patch structure varies only minimally if the substrate is reduced to only a rectangular region slightly larger than the patch. Thus, the run time per frequency point may be drastically reduced by using a smaller section of substrate. The entire substrate, however, must be modeled when the field pattern is desired, and this is made clear by the different patterns obtained for the two different size substrates. Considerable computing time is saved because only one subsection along the  $z$  direction is required.

The success of this technique for accurately calculating the performance of finite size antennas on dielectrics opens the door for studying many more complicated structures, such as multilayer configurations of [23], and mutual coupling between two or more patches [24].

#### REFERENCES

- [1] D. E. Livesay and K. M. Chen, "Electromagnetic fields induced inside arbitrarily shaped biological bodies," *IEEE Trans. Microwave Theory Tech.*, vol. MTT-22, pp. 1273-1280, Dec. 1974.
- [2] G. W. Hohmann, "Three-dimensional induced polarization and induced electromagnetic modeling," *Geophys.*, vol. 40, pp. 309-324, Apr. 1975.
- [3] M. J. Hagmann, O. P. Gandhi, and C. H. Durney, "Numerical calculation of electromagnetic energy deposition for a realistic model of man," *IEEE Trans. Microwave Theory Tech.*, vol. MTT-27, pp. 804-809, Sept. 1979.
- [4] T. K. Sarkar, E. Arvas, and S. Ponnappalli, "Electromagnetic scattering from dielectric bodies," *IEEE Trans. Antennas Propagat.*, vol. AP-37, pp. 673-676, May 1989.
- [5] D. H. Schaubert, D. R. Wilton, and A. W. Glisson, "A tetrahedral modeling method for electromagnetic scattering by arbitrarily shaped inhomogeneous dielectric bodies," *IEEE Trans. Antennas Propagat.*, vol. AP-32, pp. 77-85, Jan. 1984.
- [6] M. F. Catedra, E. Gago, and L. Nüño, "A numerical scheme to obtain the RCS of three-dimensional bodies of resonant size using the conjugate gradient method and the fast Fourier transform," *IEEE Trans. Antennas Propagat.*, vol. 37, pp. 528-537, May 1989.
- [7] T. K. Sarkar and E. Arvas, "Scattering cross section of composite conducting and lossy dielectric bodies," *Proc. IEEE*, vol. 77, pp. 788-795, May 1989.
- [8] — "An integral equation approach to the analysis of finite microstrip antennas; volume/surface formulation," *IEEE Trans. Antennas Propagat.*, vol. AP-38, pp. 305-312, Mar. 1990.
- [9] T. K. Sarkar, S. M. Rao, and A. R. Djordjević, "Electromagnetic scattering and radiation from finite microstrip structures," *IEEE Trans. Microwave Theory Tech.*, vol. 38, pp. 1568-1575, Nov. 1990.
- [10] J. Huang, "The finite ground plane effect on the microstrip antenna radiation patterns," *IEEE Trans. Antennas Propagat.*, vol. AP-31, pp. 649-653, July 1983.
- [11] H. Massoudi, C. H. Durney, and M. F. Iskander, "Limitations of the cubical block model of man in calculating SAR distributions," *IEEE Trans. Microwave Theory Tech.*, vol. MTT-32, pp. 746-752, Aug. 1984.
- [12] M. J. Hagmann, "Comments on 'Limitations of the cubical block model of man in calculating SAR distributions'," *IEEE Trans. Microwave Theory Tech.*, vol. MTT-33, pp. 347-350, Apr. 1985.

- [13] N. Jaachimowicz and C. Pichot, "Comparison of three integral formulations of the 2-D TE scattering problem," *IEEE Trans. Microwave Theory Tech.*, vol. 38, pp. 178-185, Feb. 1990.
- [14] B. J. Rubin and S. Daijavad, "Radiation and scattering from structures involving finite-size dielectric regions," *IEEE Trans. Antennas Propagat.*, vol. 38, pp. 1863-1873, Nov. 1990.
- [15] B. J. Rubin, "An electromagnetic approach for modeling high-performance computer modules," *IBM J. Res. Develop.*, vol. 34, pp. 585-600, July 1990.
- [16] B. J. Rubin, R. A. York, and R. C. Compton, "Accurate approach for modeling microstrip patch antennas," in *15th Int. Conf. Infrared and Millimeter Waves*, Orlando, FL, pp. 605-607, Dec. 1990.
- [17] B. J. Rubin, "Electromagnetic modeling of waveguides involving finite-size dielectric regions," *IEEE Trans. Microwave Theory Tech.*, vol. 38, pp. 807-812, June 1990.
- [18] R. F. Harrington, *Field Computation by Moment Methods*. New York: Macmillan, 1968.
- [19] R. W. Dearnley and A. R. F. Barel, "A broad-band transmission line model for a rectangular microstrip antenna," *IEEE Trans. Antennas Propagat.*, vol. 37, pp. 6-15, Jan. 1989.
- [20] K. Antoszkiewicz and L. Shafai, "Impedance characteristic of circular microstrip patches," *IEEE Trans. Antennas Propagat.*, vol. 38, pp. 942-946, June 1990.
- [21] D. R. Jackson, private communication.
- [22] D. H. Schaubert and K. S. Yngvesson, "Experimental study of a microstrip array on high-permittivity substrate," *IEEE Trans. Antennas Propagat.*, vol. AP-34, pp. 92-97, Jan. 1986.
- [23] D. R. Jackson and N. G. Alexopoulos, "Analysis of planar strip geometries in a substrate-superstrate configuration," *IEEE Trans. Antennas Propagat.*, vol. AP-34, pp. 1430-1438, Dec. 1986.
- [24] D. M. Pozar, "Input impedance and mutual coupling of rectangular microstrip antennas," *IEEE Trans. Antennas Propagat.*, vol. AP-30, pp. 1191-1196, Nov. 1982.

## On Internal Higher Order Mode Coupling in Slot Arrays

Sembiam R. Rengarajan and Daniel D. Nardi

**Abstract**—Internal higher order mode coupling between adjacent longitudinal radiating slots cut in a broad wall of a rectangular waveguide is examined rigorously. Method of moments solutions to pertinent coupled integral equations are investigated. Higher order mode coupling effects on amplitude and phase of the aperture electric field are studied as a function of waveguide and slot parameters. It is shown that higher order mode coupling effects are accounted for, to a substantial extent in standard-height waveguides, and almost completely in reduced height waveguides, by including the  $TE_{20}$  mode coupling in the analysis.

### INTRODUCTION

Waveguide-fed slot arrays have been investigated extensively in the literature. External mutual coupling effect was taken into account in Elliott's design procedure for an array of longitudinal slots in rectangular waveguides [1]. Later, Elliott and O'Loughlin modified the design procedure for introducing the internal mutual coupling via the  $TE_{20}$  mode [2]. By comparing the data obtained from two designs, with and without the  $TE_{20}$  mode internal coupling, they concluded that the  $TE_{20}$  mode coupling effects are ignorable for full-height guide, marginally detectable for half-height guide, but significant for quarter-height guide. However, they did

not investigate the error introduced due to the neglect of higher order modes other than  $TE_{20}$ . Recently, Rengarajan investigated higher order mode coupling effects between coupling slots in the feeding waveguide of a planar slot array [3]. A method-of-moments solution to the pertinent coupled integral equations was studied in that paper. Two types of coupling slots were considered in [3]. Internal higher order mode coupling can affect the sidelobe level and input voltage standing-wave ratio of high performance slot arrays. The objective of this communication is to investigate the internal higher order mode coupling between adjacent radiating elements in a longitudinal slot array. The presence of external mutual coupling may affect the extent of internal higher order mode coupling in this problem with respect to that in [3]. For this study, a rectangular waveguide with three radiating slots having equal values for magnitude of offsets but alternating positive and negative offsets with respect to the center line of the waveguide, a matched generator, and a matched load are considered. The central slot experiences internal coupling from two adjacent slots and, hence, this model is adequate for investigating the higher order mode coupling in slot arrays. The results to be presented here provide a sound theoretical basis for Elliott and O'Loughlin's idea to include the  $TE_{20}$  mode contribution to internal mutual coupling [2].

### II. METHOD OF ANALYSIS

Fig. 1 shows the geometry of the problem. Three longitudinal radiating slots are cut in the broad wall of a rectangular waveguide of inner dimensions  $a$ ,  $b$ , and wall thickness  $t$ . Each slot has a length  $2l$ , width  $w$ , and an offset from the center line of magnitude  $\delta$ . A  $TE_{10}$  mode matched source excites the slots from one end of the waveguide with the other end terminated in a matched load. The broad wall containing the slots is assumed to be extending to an infinite ground plane. It is assumed that the slots are narrow so that the longitudinal component of the aperture electric field may be ignored. Enforcing the continuity of the longitudinal magnetic field across each of the six apertures yields six coupled integral equations in terms of six unknown aperture electric fields. This procedure is similar to the analysis technique employed in [3]-[8]. The integral equations have been solved by a global sinusoidal Galerkin technique which generally assures an accurate solution for slots near resonance with a few terms of expansion functions for each aperture field. This method has been employed successfully previously for coupling and radiating slot problems [3]-[8]. The application of the global Galerkin type method of moments reduces the coupled integral equations to the following matrix equations:

$$\begin{bmatrix} [Y_{11}] & [Y_{12}] & [G^{12}] & [0] & [G^{13}] & [0] \\ [Y_{21}] & [Y_{22}] & [0] & [P^{12}] & [0] & [P^{13}] \\ [G^{21}] & [0] & [Y'_{11}] & [Y'_{12}] & [G^{23}] & [0] \\ [0] & [P^{21}] & [Y'_{21}] & [Y'_{22}] & [0] & [P^{23}] \\ [G^{31}] & [0] & [G^{32}] & [0] & [Y''_{11}] & [Y''_{12}] \\ [0] & [P^{31}] & [0] & [P^{32}] & [Y''_{21}] & [Y''_{22}] \end{bmatrix} \begin{bmatrix} A_1 \\ A'_1 \\ A_2 \\ A'_2 \\ A_3 \\ A'_3 \end{bmatrix} = \begin{bmatrix} I_1 \\ 0 \\ I_2 \\ 0 \\ I_3 \\ 0 \end{bmatrix} \quad (1)$$

Manuscript received July 9, 1990; revised December 11, 1990. This work was supported in part by the Hughes Aircraft Company, and by the University of California, Los Angeles.

The authors are with the Department of Electrical and Computer Engineering, California State University, Northridge, CA 91330.

IEEE Log Number 9143725.